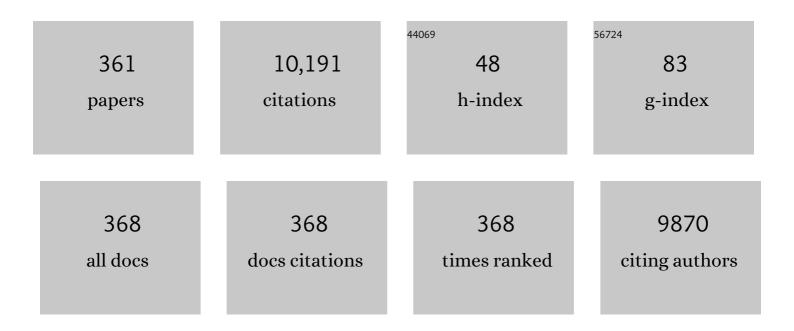
List of Publications by Year in descending order

Source: https://exaly.com/author-pdf/4021042/publications.pdf Version: 2024-02-01



#	Article	IF	CITATIONS
1	Support nanostructure boosts oxygen transfer to catalytically active platinum nanoparticles. Nature Materials, 2011, 10, 310-315.	27.5	748
2	Counting electrons on supported nanoparticles. Nature Materials, 2016, 15, 284-288.	27.5	469
3	Creating single-atom Pt-ceria catalysts by surface step decoration. Nature Communications, 2016, 7, 10801.	12.8	388
4	Maximum Nobleâ€Metal Efficiency in Catalytic Materials: Atomically Dispersed Surface Platinum. Angewandte Chemie - International Edition, 2014, 53, 10525-10530.	13.8	384
5	In Situ and Theoretical Studies for the Dissociation of Water on an Active Ni/CeO ₂ Catalyst: Importance of Strong Metal–Support Interactions for the Cleavage of O–H Bonds. Angewandte Chemie - International Edition, 2015, 54, 3917-3921.	13.8	205
6	Direct Conversion of Methane to Methanol on Ni-Ceria Surfaces: Metal–Support Interactions and Water-Enabled Catalytic Conversion by Site Blocking. Journal of the American Chemical Society, 2018, 140, 7681-7687.	13.7	141
7	Inâ€Situ Investigation of Methane Dry Reforming on Metal/Ceria(111) Surfaces: Metal–Support Interactions and Câ^'H Bond Activation at Low Temperature. Angewandte Chemie - International Edition, 2017, 56, 13041-13046.	13.8	120
8	Ceria reoxidation by CO2: A model study. Journal of Catalysis, 2010, 275, 181-185.	6.2	115
9	Cerium oxide stoichiometry alteration via Sn deposition: Influence of temperature. Journal of Electron Spectroscopy and Related Phenomena, 2009, 169, 20-25.	1.7	111
10	Water Chemistry on Model Ceria and Pt/Ceria Catalysts. Journal of Physical Chemistry C, 2012, 116, 12103-12113.	3.1	108
11	The influence of particle size on CO adsorption on Pd/alumina model catalysts. Surface Science, 1994, 313, 99-106.	1.9	105
12	Epitaxial Cubic Ce ₂ O ₃ Films via Ce–CeO ₂ Interfacial Reaction. Journal of Physical Chemistry Letters, 2013, 4, 866-871.	4.6	99
13	Atomically Dispersed Pd, Ni, and Pt Species in Ceria-Based Catalysts: Principal Differences in Stability and Reactivity. Journal of Physical Chemistry C, 2016, 120, 9852-9862.	3.1	99
14	Electrifying model catalysts for understanding electrocatalytic reactions in liquid electrolytes. Nature Materials, 2018, 17, 592-598.	27.5	89
15	Adsorption sites, metal-support interactions, and oxygen spillover identified by vibrational spectroscopy of adsorbed CO: A model study on Pt/ceria catalysts. Journal of Catalysis, 2012, 289, 118-126.	6.2	88
16	Epitaxial growth of continuous CeO2(111) ultra-thin films on Cu(111). Thin Solid Films, 2008, 516, 6120-6124.	1.8	85
17	Water interaction with CeO2(1 1 1)/Cu(1 1 1) model catalyst surface. Catalysis Today, 2012, 181, 124-132.	4.4	85
18	Methanol decomposition on Pd(111) single crystal surfaces. Surface Science, 1990, 238, L457-L462.	1.9	84

#	Article	IF	CITATIONS
19	Platinum-Doped CeO ₂ Thin Film Catalysts Prepared by Magnetron Sputtering. Langmuir, 2010, 26, 12824-12831.	3.5	84
20	Oxide-based nanomaterials for fuel cell catalysis: the interplay between supported single Pt atoms and particles. Catalysis Science and Technology, 2017, 7, 4315-4345.	4.1	84
21	Thermodynamic, electronic and structural properties of Cu/CeO \$_2\$2 surfaces and interfaces from first-principles DFT+U calculations. Journal of Chemical Physics, 2010, 133, 234705.	3.0	83
22	Ordered Phases of Reduced Ceria As Epitaxial Films on Cu(111). Journal of Physical Chemistry C, 2014, 118, 357-365.	3.1	83
23	Ambient pressure XPS and IRRAS investigation of ethanol steam reforming on Ni–CeO ₂ (111) catalysts: an in situ study of C–C and O–H bond scission. Physical Chemistry Chemical Physics, 2016, 18, 16621-16628.	2.8	83
24	Adjusting Morphology and Surface Reduction of CeO2(111) Thin Films on Cu(111). Journal of Physical Chemistry C, 2011, 115, 7496-7503.	3.1	82
25	Unraveling the surface state and composition of highly selective nanocrystalline Ni–Cu alloy catalysts for hydrodeoxygenation of HMF. Catalysis Science and Technology, 2017, 7, 1735-1743.	4.1	82
26	The effect of sulfur dioxide on the activity of hierarchical Pd-based catalysts in methane combustion. Applied Catalysis B: Environmental, 2017, 202, 72-83.	20.2	80
27	Methanol adsorption on a CeO2(1 1 1)/Cu(1 1 1) thin film model catalyst. Surface Science, 2009, 603, 1087-1092.	1.9	79
28	Activity of oxygen reduction reaction on small amount of amorphous CeO promoted Pt cathode for fuel cell application. Electrochimica Acta, 2011, 56, 3874-3883.	5.2	75
29	A resonant photoelectron spectroscopy study of Sn(O _{<i>x</i>}) doped CeO ₂ catalysts. Surface and Interface Analysis, 2008, 40, 225-230.	1.8	74
30	<i>In Situ</i> Imaging of Cu ₂ 0 under Reducing Conditions: Formation of Metallic Fronts by Mass Transfer. Journal of the American Chemical Society, 2013, 135, 16781-16784.	13.7	74
31	In Situ DRIFTS and NAP-XPS Exploration of the Complexity of CO ₂ Hydrogenation over Size-Controlled Pt Nanoparticles Supported on Mesoporous NiO. Journal of Physical Chemistry C, 2018, 122, 5553-5565.	3.1	72
32	Defect-induced dissociation of CO on palladium. Surface Science, 1991, 245, 233-243.	1.9	68
33	A route to continuous ultra-thin cerium oxide films on Cu(1 1 1). Surface Science, 2009, 603, 3382-3388.	1.9	67
34	The influence of particle size on CO oxidation on Pd/alumina model catalyst. Surface Science, 1995, 331-333, 173-177.	1.9	65
35	Growth of ultra-thin cerium oxide layers on Cu(1 1 1). Applied Surface Science, 2007, 254, 153-155.	6.1	64
36	CO disproportionation over supported Pd particles: a TPD and static SIMS study. Surface Science, 1990, 238, 75-82.	1.9	62

#	Article	IF	CITATIONS
37	Chemisorptional behaviour of Pd small supported particles depending on size and structure: TDS, SSIMS and TEM investigation. Surface Science, 1985, 152-153, 603-614.	1.9	61
38	Acceptor-like behavior of reducing gases on the surface of n-type In2O3. Applied Surface Science, 2004, 227, 122-131.	6.1	61
39	Reactivity of atomically dispersed Pt ²⁺ species towards H ₂ : model Pt–CeO ₂ fuel cell catalyst. Physical Chemistry Chemical Physics, 2016, 18, 7672-7679.	2.8	61
40	Palladium interaction with CeO ₂ , Sn–Ce–O and Ga–Ce–O layers. Journal of Physics Condensed Matter, 2009, 21, 055005.	1.8	60
41	Interaction of Au with CeO2(111): A photoemission study. Journal of Chemical Physics, 2009, 130, 034703.	3.0	60
42	A resonant photoemission applied to cerium oxide based nanocrystals. Nanotechnology, 2009, 20, 215706.	2.6	58
43	Electronic Structure of Magnesiaâ^'Ceria Model Catalysts, CO ₂ Adsorption, and CO ₂ Activation: A Synchrotron Radiation Photoelectron Spectroscopy Study. Journal of Physical Chemistry C, 2011, 115, 8716-8724.	3.1	57
44	Core and Valence Band Photoemission Spectroscopy of Well-Ordered Ultrathin TiOxFilms on Pt(111). Journal of Physical Chemistry C, 2007, 111, 869-876.	3.1	56
45	Adsorption of Histidine and Histidine-Containing Peptides on Au(111). Langmuir, 2010, 26, 8606-8613.	3.5	54
46	Pt–CeO thin film catalysts for PEMFC. Catalysis Today, 2015, 240, 236-241.	4.4	52
47	High efficiency of Pt2+- CeO2 novel thin film catalyst as anode for proton exchange membrane fuel cells. Applied Catalysis B: Environmental, 2016, 197, 262-270.	20.2	52
48	Bulk Hydroxylation and Effective Water Splitting by Highly Reduced Cerium Oxide: The Role of O Vacancy Coordination. ACS Catalysis, 2018, 8, 4354-4363.	11.2	52
49	Investigation of gas sensing mechanism of SnO2 based chemiresistor using near ambient pressure XPS. Surface Science, 2018, 677, 284-290.	1.9	51
50	Optimization of ionomer-free ultra-low loading Pt catalyst for anode/cathode of PEMFC via magnetron sputtering. International Journal of Hydrogen Energy, 2019, 44, 19344-19356.	7.1	51
51	Stabilization of Small Platinum Nanoparticles on Pt–CeO ₂ Thin Film Electrocatalysts During Methanol Oxidation. Journal of Physical Chemistry C, 2016, 120, 19723-19736.	3.1	50
52	Atomic species identification at the (101) anatase surface by simultaneous scanning tunnelling and atomic force microscopy. Nature Communications, 2015, 6, 7265.	12.8	49
53	Proton exchange membrane fuel cell made of magnetron sputtered Pt–CeO and Pt–Co thin film catalysts. Journal of Power Sources, 2015, 273, 105-109.	7.8	47
54	The surface diffusion in CO oxidation on small supported Pd particles: Experimental evidence. Surface Science, 1986, 166, L115-L118.	1.9	46

#	Article	IF	CITATIONS
55	Study of CO desorption and dissociation on Rh surfaces. Surface Science, 1995, 331-333, 105-109.	1.9	45
56	Hydrogen spillover monitored by resonant photoemission spectroscopy. Journal of Catalysis, 2012, 285, 6-9.	6.2	45
57	A photoemission study of the interaction of Ga with CeO2(111) thin films. Applied Surface Science, 2008, 254, 6860-6864.	6.1	44
58	Structure-Dependent Dissociation of Water on Cobalt Oxide. Journal of Physical Chemistry Letters, 2018, 9, 2763-2769.	4.6	44
59	Sn interaction with the CeO2(111) system: Bimetallic bonding and ceria reduction. Applied Surface Science, 2008, 254, 4375-4379.	6.1	42
60	Spectroscopic Understanding of SnO2 and WO3 Metal Oxide Surfaces with Advanced Synchrotron Based; XPS-UPS and Near Ambient Pressure (NAP) XPS Surface Sensitive Techniques for Gas Sensor Applications under Operational Conditions. Sensors, 2019, 19, 4737.	3.8	42
61	Methanol decomposition on oxygen precovered and atomically clean Pd(111) single crystal surfaces. Surface Science, 1991, 251-252, 1117-1122.	1.9	40
62	Influence of substrate structure on activity of alumina supported Pd particles: CO adsorption and oxidation. Surface Science, 1996, 365, 69-77.	1.9	40
63	Photoemission Spectroscopy Study of Cu/CeO ₂ Systems:  Cu/CeO ₂ Nanosized Catalyst and CeO ₂ (111)/Cu(111) Inverse Model Catalyst. Journal of Physical Chemistry C, 2008, 112, 3751-3758.	3.1	40
64	Distinct Physicochemical Properties of the First Ceria Monolayer on Cu(111). Journal of Physical Chemistry C, 2012, 116, 6677-6684.	3.1	40
65	Quantitative Analysis of the Oxidation State of Cobalt Oxides by Resonant Photoemission Spectroscopy. Journal of Physical Chemistry Letters, 2019, 10, 6129-6136.	4.6	39
66	The Electronic Structure and Adsorption Geometry of <scp>l</scp> -Histidine on Cu(110). Journal of Physical Chemistry B, 2008, 112, 13655-13660.	2.6	38
67	lonomer content effect on charge and gas transport in the cathode catalyst layer of proton-exchange membrane fuel cells. Journal of Power Sources, 2021, 490, 229531.	7.8	38
68	Size effect study of carbon monoxide oxidation by Rh surfaces. Surface Science, 1996, 352-354, 305-309.	1.9	37
69	Copper-ceria interaction: A combined photoemission and DFT study. Applied Surface Science, 2013, 267, 12-16.	6.1	37
70	Mechanistic Insights of Ethanol Steam Reforming over Ni–CeO _{<i>x</i>} (111): The Importance of Hydroxyl Groups for Suppressing Coke Formation. Journal of Physical Chemistry C, 2015, 119, 18248-18256.	3.1	37
71	Adsorption of CO on Small Supported Rhodium Particles: SSIMS and TPD Study. Journal of Catalysis, 1993, 143, 492-498.	6.2	36
72	Functionalization of Oxide Surfaces through Reaction with 1,3-Dialkylimidazolium Ionic Liquids. Journal of Physical Chemistry Letters, 2013, 4, 30-35.	4.6	36

#	Article	IF	CITATIONS
73	Magnetron sputtered Ir thin film on TiC-based support sublayer as low-loading anode catalyst for proton exchange membrane water electrolysis. International Journal of Hydrogen Energy, 2016, 41, 15124-15132.	7.1	36
74	Mechanism of non-evaporable getter activation XPS and static SIMS study of Zr44V56 alloy. Vacuum, 2003, 71, 317-322.	3.5	35
75	Miniature electron bombardment evaporation source: evaporation rate measurement. European Physical Journal D, 1997, 47, 261-268.	0.4	34
76	Methanol Adsorption and Decomposition on Pt/CeO ₂ (111)/Cu(111) Thin Film Model Catalyst. Langmuir, 2010, 26, 13333-13341.	3.5	34
77	Crystallographic structure and chemisorption activity of palladium/mica model catalysts III. Static secondary ion mass spectrometry study of CO chemisorption on small palladium particles. Journal of Catalysis, 1986, 97, 448-455.	6.2	33
78	Sn–CeO2 thin films prepared by rf magnetron sputtering: XPS and SIMS study. Applied Surface Science, 2009, 255, 6656-6660.	6.1	33
79	Adsorption and Decomposition of Formic Acid on Model Ceria and Pt/Ceria Catalysts. Journal of Physical Chemistry C, 2013, 117, 12483-12494.	3.1	33
80	Structural and electronic properties of manganese-doped Bi ₂ Te ₃ epitaxial layers. New Journal of Physics, 2015, 17, 013028.	2.9	33
81	Surface composition of magnetron sputtered Pt-Co thin film catalyst for proton exchange membrane fuel cells. Applied Surface Science, 2016, 365, 245-251.	6.1	33
82	Roomâ€Temperature Atomic‣ayerâ€Deposited Al ₂ O ₃ Improves the Efficiency of Perovskite Solar Cells over Time. ChemSusChem, 2018, 11, 3640-3648.	6.8	33
83	Effect of ZnO on acid–base properties and catalytic performances of ZnO/ZrO ₂ –SiO ₂ catalysts in 1,3-butadiene production from ethanol–water mixture. Catalysis Science and Technology, 2019, 9, 3964-3978.	4.1	33
84	CO oxidation over small Pd particle model catalysts. A static secondary ion mass spectrometry study. Journal of the Chemical Society, Faraday Transactions, 1990, 86, 2749.	1.7	32
85	Au ⁺ and Au ³⁺ ions in CeO ₂ rf-sputtered thin films. Journal Physics D: Applied Physics, 2009, 42, 115301.	2.8	32
86	Formation of alumina–ceria mixed oxide in model systems. Applied Surface Science, 2011, 257, 3682-3687.	6.1	32
87	In situ probing of magnetron sputtered Pt-Ni alloy fuel cell catalysts during accelerated durability test using EC-AFM. Electrochimica Acta, 2017, 245, 760-769.	5.2	32
88	Steady carbon formation during CO oxidation over small Pd particles: A static SIMS study. Surface Science, 1987, 186, L541-L547.	1.9	31
89	Nitridation of GaAs(1 0 0) substrates and Ga/GaAs systems studied by XPS spectroscopy. Applied Surface Science, 2003, 212-213, 614-618.	6.1	31
90	Bonding at the organic/metal interface: Adenine to Cu(110). Physical Review B, 2009, 79, .	3.2	31

#	Article	IF	CITATIONS
91	Magnetron sputtered thin-film vertically segmented Pt-Ir catalyst supported on TiC for anode side of proton exchange membrane unitized regenerative fuel cells. International Journal of Hydrogen Energy, 2019, 44, 16087-16098.	7.1	31
92	Adsorption Structure of Glycyl-Glycine on Cu(110). Journal of Physical Chemistry C, 2010, 114, 10922-10931.	3.1	30
93	Electrochemical activity of the polycrystalline cerium oxide films for hydrogen peroxide detection. Applied Surface Science, 2019, 488, 351-359.	6.1	30
94	CO dissociation and oxidation on small supported rhodium particles: SSIMS and TPR study. Catalysis Letters, 1993, 21, 175-182.	2.6	29
95	Structural and temperature-related disordering studies of Cu6PS5I amorphous thin films. Thin Solid Films, 2012, 520, 1729-1733.	1.8	29
96	Bonding of Histidine to Cerium Oxide. Journal of Physical Chemistry B, 2013, 117, 9182-9193.	2.6	29
97	Experimental and Theoretical Investigation of the Restructuring Process Induced by CO at Near Ambient Pressure: Pt Nanoclusters on Graphene/Ir(111). ACS Nano, 2017, 11, 1041-1053.	14.6	29
98	Synchrotron radiation photoemission study of indium oxide surface prepared by spray pyrolysis method. Applied Surface Science, 2005, 243, 335-344.	6.1	28
99	Phosphorus poisoning during wet oxidation of methane over Pd@CeO2/graphite model catalysts. Applied Catalysis B: Environmental, 2016, 197, 271-279.	20.2	28
100	Comparison of Antibacterial Mode of Action of Silver Ions and Silver Nanoformulations With Different Physico-Chemical Properties: Experimental and Computational Studies. Frontiers in Microbiology, 2021, 12, 659614.	3.5	28
101	Interaction of ultrathin nickel oxide films with single-crystal zirconia and alumina surfaces. Surface and Interface Analysis, 2002, 34, 545-549.	1.8	27
102	The adsorption of adenine on mineral surfaces: Iron pyrite and silicon dioxide. Surface Science, 2007, 601, 1973-1980.	1.9	27
103	Preparation of Magnetron Sputtered Thin Cerium Oxide Films with a Large Surface on Silicon Substrates Using Carbonaceous Interlayers. ACS Applied Materials & Interfaces, 2014, 6, 1213-1218.	8.0	27
104	Efficient Ceria–Platinum Inverse Catalyst for Partial Oxidation of Methanol. Langmuir, 2016, 32, 6297-6309.	3.5	27
105	Valence band and band gap photoemission study of (111) In2O3 epitaxial films under interactions with oxygen, water and carbon monoxide. Surface Science, 2007, 601, 5585-5594.	1.9	26
106	Pt ^{2 + , 4+} ions in CeO ₂ rfâ€sputtered thin films. Surface and Interface Analysis, 2010, 42, 882-885.	1.8	25
107	Surface sites on Pt–CeO ₂ mixed oxide catalysts probed by CO adsorption: a synchrotron radiation photoelectron spectroscopy study. Physical Chemistry Chemical Physics, 2014, 16, 24747-24754.	2.8	25
108	Impact of Rh–CeO interaction on CO oxidation mechanisms. Applied Surface Science, 2015, 332, 747-755.	6.1	25

#	Article	IF	CITATIONS
109	In situ electrochemical AFM monitoring of the potential-dependent deterioration of platinum catalyst during potentiodynamic cycling. Ultramicroscopy, 2018, 187, 64-70.	1.9	25
110	Pt–CeO ₂ Coating of Carbon Nanotubes Grown on Anode Gas Diffusion Layer of the Polymer Electrolyte Membrane Fuel Cell. Journal of Nanoscience and Nanotechnology, 2011, 11, 5062-5067.	0.9	24
111	Revealing chemical ordering in Pt–Co nanoparticles using electronic structure calculations and X-ray photoelectron spectroscopy. Physical Chemistry Chemical Physics, 2015, 17, 28298-28310.	2.8	24
112	RHEED study of the growth of cerium oxide on Cu(1 1 1). Applied Surface Science, 2012, 259, 34-38.	6.1	23
113	In-situ electrochemical atomic force microscopy study of aging of magnetron sputtered Pt-Co nanoalloy thin films during accelerated degradation test. Electrochimica Acta, 2016, 211, 52-58.	5.2	23
114	Interplay between the metal-support interaction and stability in Pt/Co ₃ O ₄ (111) model catalysts. Journal of Materials Chemistry A, 2018, 6, 23078-23086.	10.3	23
115	SRPES investigation of tungsten oxide in different oxidation states. Surface Science, 2006, 600, 1624-1627.	1.9	22
116	Interface termination and band alignment of epitaxially grown alumina films on Cu–Al alloy. Journal of Applied Physics, 2008, 103, 033707.	2.5	22
117	Enhanced reactivity of Pt nanoparticles supported on ceria thin films during ethylenedehydrogenation. Physical Chemistry Chemical Physics, 2011, 13, 253-261.	2.8	22
118	Interactions of Imidazoliumâ€Based Ionic Liquids with Oxide Surfaces Controlled by Alkyl Chain Functionalization. ChemPhysChem, 2013, 14, 3673-3677.	2.1	22
119	Subpixel detection in video RHEED image analysis. Thin Solid Films, 1995, 259, 65-69.	1.8	21
120	Electronic properties of Sn/Pd intermetallic compounds on Pd(110). Surface Science, 2005, 595, 138-150.	1.9	21
121	Mechanism of Sulfur Poisoning and Storage: Adsorption and Reaction of SO ₂ with Stoichiometric and Reduced Ceria Films on Cu(111). Journal of Physical Chemistry C, 2011, 115, 19872-19882.	3.1	21
122	CO and methanol adsorption on (2 × 1)Pt(110) and ionâ€eroded Pt(111) model catalysts. Surface and Interface Analysis, 2011, 43, 1325-1331.	1.8	21
123	Growth and composition of nanostructured and nanoporous cerium oxide thin films on a graphite foil. Nanoscale, 2015, 7, 4038-4047.	5.6	21
124	Experimental and Theoretical Study on the Electronic Interaction between Rh Adatoms and CeOx Substrate in Dependence on a Degree of Cerium Oxide Reduction. Journal of Physical Chemistry C, 2016, 120, 5468-5476.	3.1	21
125	Oxygen partial pressure dependence of surface space charge formation in donor-doped SrTiO ₃ . APL Materials, 2017, 5, 056106.	5.1	21
126	Ultimate dispersion of metallic and ionic platinum on ceria. Journal of Materials Chemistry A, 2019, 7, 13019-13028.	10.3	21

#	Article	IF	CITATIONS
127	Cobalt Oxide-Supported Pt Electrocatalysts: Intimate Correlation between Particle Size, Electronic Metal–Support Interaction and Stability. Journal of Physical Chemistry Letters, 2020, 11, 8365-8371.	4.6	21
128	All-Oxide p–n Junction Thermoelectric Generator Based on SnO <i>_x</i> and ZnO Thin Films. ACS Applied Materials & Interfaces, 2021, 13, 35187-35196.	8.0	21
129	Study of CO interaction with alumina-supported Pd particles. Surface Science, 1997, 377-379, 644-649.	1.9	20
130	CO diffusion over the alumina support of Pd particle model catalysts. Surface Science, 1998, 398, 117-124.	1.9	20
131	Nanostructured Pt–CeO2 thin film catalyst grown on graphite foil by magnetron sputtering. Applied Surface Science, 2013, 267, 119-123.	6.1	20
132	Comment on "Ordered Phases of Reduced Ceria as Epitaxial Films on Cu(111)― Journal of Physical Chemistry C, 2014, 118, 5058-5059.	3.1	20
133	Altering properties of cerium oxide thin films by Rh doping. Materials Research Bulletin, 2015, 67, 5-13.	5.2	20
134	Controlling Heteroepitaxy by Oxygen Chemical Potential: Exclusive Growth of (100) Oriented Ceria Nanostructures on Cu(111). Journal of Physical Chemistry C, 2016, 120, 4895-4901.	3.1	20
135	Charge transfer and spillover phenomena in ceria-supported iridium catalysts: A model study. Journal of Chemical Physics, 2019, 151, 204703.	3.0	20
136	Study of the growth of rhodium particles on different substrates. Thin Solid Films, 1995, 260, 252-258.	1.8	19
137	Static SIMS study of Ti, Zr, V and Ti–Zr–V NEG activation. Vacuum, 2003, 71, 323-327.	3.5	19
138	A study of tungsten oxide nanowires self-organized on mica support. Nanotechnology, 2009, 20, 445604.	2.6	19
139	Photoemission study of the tin doped cerium oxide thin films prepared by RF magnetron sputtering. Thin Solid Films, 2010, 518, 2206-2209.	1.8	19
140	Modification of terminating species and band alignment at the interface between alumina films and metal single crystals. Surface Science, 2010, 604, 2150-2156.	1.9	19
141	In situ growth of epitaxial cerium tungstate (100) thin films. Physical Chemistry Chemical Physics, 2011, 13, 7083.	2.8	19
142	Methanol oxidation on sputter-coated platinum oxide catalysts. International Journal of Hydrogen Energy, 2016, 41, 265-275.	7.1	19
143	Unraveling the resistive switching effect in ZnO/0.5Ba(Zr 0.2 Ti 0.8)O 3 -0.5(Ba 0.7 Ca 0.3)TiO 3 heterostructures. Applied Surface Science, 2017, 400, 453-460.	6.1	19
144	Photoemission Study of Thymidine Adsorbed on Au(111) and Cu(110). Journal of Physical Chemistry C, 2010, 114, 15036-15041.	3.1	18

#	Article	IF	CITATIONS
145	Alcohol Dehydration on Monooxo Wâ•O and Dioxo Oâ•Wâ•O Species. Journal of Physical Chemistry Letters, 2012, 3, 2168-2172.	4.6	18
146	SO ₂ Decomposition on Pt/CeO ₂ (111) Model Catalysts: On the Reaction Mechanism and the Influence of H ₂ and CO. Journal of Physical Chemistry C, 2012, 116, 10959-10967.	3.1	18
147	Adsorption of Cytosine and AZA Derivatives of Cytidine on Au Single Crystal Surfaces. Journal of Physical Chemistry C, 2013, 117, 18423-18433.	3.1	18
148	Polarity driven morphology of CeO2(100) islands on Cu(111). Applied Surface Science, 2013, 285, 766-771.	6.1	18
149	Atomic and Electronic Structure of V–Rh(110) Near-Surface Alloy. Journal of Physical Chemistry C, 2013, 117, 12679-12688.	3.1	18
150	High low-temperature CO oxidation activity of platinum oxide prepared by magnetron sputtering. Applied Surface Science, 2015, 345, 319-328.	6.1	18
151	Characterization of thin CeO2 films electrochemically deposited on HOPG. Applied Surface Science, 2015, 350, 142-148.	6.1	18
152	Reduction of Pt2+ species in model Pt–CeO2 fuel cell catalysts upon reaction with methanol. Applied Surface Science, 2016, 387, 674-681.	6.1	18
153	Efficient Ptâ€C MEA for PEMFC with Low Platinum Content Prepared by Magnetron Sputtering. Fuel Cells, 2018, 18, 51-56.	2.4	18
154	SSIMS and TDS investigation of CO adsorption on Pd(111) during CO and O2 exposure. Surface Science, 1985, 164, 209-219.	1.9	17
155	Structure of the CO bond on supported Pd particles: influence of size and surface state. Zeitschrift Für Physik D-Atoms Molecules and Clusters, 1991, 19, 361-365.	1.0	17
156	Molecular beam study of CO and O2 sticking coefficients on Rh model catalysts. Surface Science, 1997, 377-379, 813-818.	1.9	16
157	Study of InP(100) surface nitridation by x-ray photoelectron spectroscopy. Surface and Interface Analysis, 2002, 34, 712-715.	1.8	16
158	An epitaxial hexagonal tungsten bronze as precursor for WO3 nanorods on mica. Journal of Crystal Growth, 2008, 310, 3318-3324.	1.5	16
159	The interface structure and band alignment at alumina/Cu(Al) alloy interfaces—Influence of the crystallinity of alumina films. Applied Surface Science, 2010, 256, 3051-3057.	6.1	16
160	Role of Oxygen in Acetic Acid Decomposition on Pt(111). Journal of Physical Chemistry C, 2014, 118, 14316-14325.	3.1	16
161	Water Adsorption and Dissociation at Metal-Supported Ceria Thin Films: Thickness and Interface-Proximity Effects Studied with DFT+U Calculations. Journal of Physical Chemistry C, 2015, 119, 2537-2544.	3.1	16
162	Candle Soot as Efficient Support for Proton Exchange Membrane Fuel Cell Catalyst. Fuel Cells, 2016, 16, 652-655.	2.4	16

#	Article	IF	CITATIONS
163	Micro-contacted self-assembled tungsten oxide nanorods for hydrogen gas sensing. International Journal of Hydrogen Energy, 2017, 42, 1344-1352.	7.1	16
164	MoSe <i>_x</i> O <i>_y</i> â€Coated 1D TiO ₂ Nanotube Layers: Efficient Interface for Lightâ€Driven Applications. Advanced Materials Interfaces, 2018, 5, 1701146.	3.7	16
165	Electrocatalysis with Atomically Defined Model Systems: Metal–Support Interactions between Pt Nanoparticles and Co3O4(111) under Ultrahigh Vacuum and in Liquid Electrolytes. Journal of Physical Chemistry C, 2018, 122, 20787-20799.	3.1	16
166	Redox Behavior of Pt/Co ₃ O ₄ (111) Model Electrocatalyst Studied by X-ray Photoelectron Spectroscopy Coupled with an Electrochemical Cell. Journal of Physical Chemistry C, 2019, 123, 8746-8758.	3.1	16
167	Unraveling the Surface Chemistry and Structure in Highly Active Sputtered Pt ₃ Y Catalyst Films for the Oxygen Reduction Reaction. ACS Applied Materials & Interfaces, 2020, 12, 4454-4462.	8.0	16
168	Activation of binary Zr–V non-evaporable getters: synchrotron radiation photoemission study. Applied Surface Science, 2005, 243, 106-112.	6.1	15
169	Guanine adsorption on the Cu(110) surface. Surface Science, 2011, 605, 361-365.	1.9	15
170	Nanometer-Range Strain Distribution in Layered Incommensurate Systems. Physical Review Letters, 2012, 109, 266102.	7.8	15
171	Characterization of Nanoporous WO3 Films Grown via Ballistic Deposition. Journal of Physical Chemistry C, 2012, 116, 10649-10655.	3.1	15
172	On the interaction of Mg with the (111) and (110) surfaces of ceria. Physical Chemistry Chemical Physics, 2012, 14, 1293-1301.	2.8	15
173	Growth of nano-porous Pt-doped cerium oxide thin films on glassy carbon substrate. Ceramics International, 2013, 39, 3765-3769.	4.8	15
174	HAXPES study of CeO thin film–silicon oxide interface. Applied Surface Science, 2014, 303, 46-53.	6.1	15
175	Structural transformations and adsorption properties of PtNi nanoalloy thin film electrocatalysts prepared by magnetron co-sputtering. Electrochimica Acta, 2017, 251, 427-441.	5.2	15
176	Rh particle growth on insulator substrates: RHEED study. Thin Solid Films, 1996, 286, 330-335.	1.8	14
177	INFLUENCE OF SURFACE STRUCTURE ON THE MECHANISM OF CO ADSORPTION AND CATALYTIC OXIDATION ON PALLADIUM. Surface Review and Letters, 1997, 04, 1353-1358.	1.1	14
178	Angle resolved photoemission study of the Ce/Pd(111) interface. Surface Science, 2006, 600, 2317-2322.	1.9	14
179	XPS study of the formation of ultrathin GaN film on GaAs(100). Applied Surface Science, 2008, 254, 4150-4153.	6.1	14
180	Pt and Sn Doped Sputtered CeO ₂ Electrodes for Fuel Cell Applications. Fuel Cells, 2010, 10, 139-144.	2.4	14

#	Article	IF	CITATIONS
181	Adsorption of 5-halouracils on Au(111). Surface Science, 2012, 606, 435-443.	1.9	14
182	Synchrotron radiation photoelectron spectroscopy study of metal-oxide thin film catalysts: Pt–CeO2 coated CNTs. Applied Surface Science, 2012, 258, 2161-2164.	6.1	14
183	PLD prepared nanostructured Pt-CeO2 thin films containing ionic platinum. Applied Surface Science, 2017, 396, 278-283.	6.1	14
184	Sputter-etching treatment of proton-exchange membranes: Completely dry thin-film approach to low-loading catalyst-coated membranes for water electrolysis. International Journal of Hydrogen Energy, 2020, 45, 20776-20786.	7.1	14
185	Sputtered Ir–Ru based catalysts for oxygen evolution reaction: Study of iridium effect on stability. International Journal of Hydrogen Energy, 2022, 47, 21033-21043.	7.1	14
186	Reflection high-energy electron diffraction study of growth and modification of small particle model catalyst: Pd on mica. Journal of Crystal Growth, 1993, 134, 75-80.	1.5	13
187	RHEED study of Pd thin film growth on α-Al2O3 substrate. Vacuum, 1998, 50, 151-155.	3.5	13
188	XPS, TDS and static SIMS studies of binary Pd/Al system properties: correlation between Pd–Al bimetallic interaction and CO adsorption. Applied Surface Science, 2005, 245, 87-93.	6.1	13
189	Structural, electronic and adsorption properties of V–Rh(111) subsurface alloy. Journal of Alloys and Compounds, 2012, 543, 189-196.	5.5	13
190	Electronic structure and bonding of small Pd clusters on stoichiometric and reduced SnO2(110) surfaces. Vacuum, 2014, 106, 86-93.	3.5	13
191	RHEED and XPS study of cerium interaction with SnO2 (110) surface. Ceramics International, 2014, 40, 323-329.	4.8	13
192	Adenine adlayers on Cu(111): XPS and NEXAFS study. Journal of Chemical Physics, 2015, 143, 174704.	3.0	13
193	Decomposition of Acetic Acid on Model Pt/CeO ₂ Catalysts: The Effect of Surface Crowding. Journal of Physical Chemistry C, 2015, 119, 13721-13734.	3.1	13
194	Influence of the Ce–F interaction on cerium photoelectron spectra in CeO F layers. Chemical Physics Letters, 2015, 639, 126-130.	2.6	13
195	Covalent versus localized nature of <mml:math xmlns:mml="http://www.w3.org/1998/Math/MathML"> <mml:mrow> <mml:mn>4</mml:mn> <mml:mi>f</mml:mi> electrons in ceria: Resonant angle-resolved photoemission spectroscopy and density functional theory. Physical Review B. 2017, 95.</mml:mrow></mml:math 	≺¦mml:m	row ₃ >
196	An experimental and theoretical study of adenine adsorption on Au(111). Physical Chemistry Chemical Physics, 2018, 20, 4688-4698.	2.8	13
197	Morphological, optical and photovoltaic characteristics of MoSe2/SiOx/Si heterojunctions. Scientific Reports, 2020, 10, 1215.	3.3	13
198	Site dependent dissociation of CO on supported Pd particle surface: A TPD study. Progress in Surface Science, 1990, 35, 175-178.	8.3	12

#	Article	IF	CITATIONS
199	Evidence for valence-charge fluctuations in the3×3â^'Pbâ^•Si(111)system. Physical Review B, 2004, 70, .	3.2	12
200	Photoemission study ofCOadsorption on orderedPbâ^•Ni(111)surface phases. Physical Review B, 2006, 74, .	3.2	12
201	A resonant photoemission study of the Ce and Ce-oxide/Pd(111) interfaces. Surface Science, 2007, 601, 4958-4965.	1.9	12
202	Interaction of tungsten with CeO ₂ (111) layers as a function of temperature: a photoelectron spectroscopy study. Journal of Physics Condensed Matter, 2011, 23, 215001.	1.8	12
203	Structural and electronic studies of supported Pt and Au epitaxial clusters on tungsten oxide surface. Vacuum, 2012, 86, 586-589.	3.5	12
204	Establishing structure-sensitivity of ceria reducibility: real-time observations of surface-hydrogen interactions. Journal of Materials Chemistry A, 2020, 8, 5501-5507.	10.3	12
205	Influence of Pt and CeO2 interaction in Pt-CeO2 electrode on anode and cathode performance for fuel cell applications. Transactions of the Materials Research Society of Japan, 2008, 33, 1101-1104.	0.2	12
206	XPS study of Pd particle growth on different alumina surfaces. Vacuum, 1998, 50, 143-145.	3.5	11
207	RHEED investigation of lattice deformations of α-Al2O3 supported Pd particles. European Physical Journal D, 1999, 9, 557-560.	1.3	11
208	Surface segregation in FeSi alloys. Surface Science, 2006, 600, 4108-4112.	1.9	11
209	The transition from the adsorbed state to a surface alloy in the Sn/Ni(111) system. Surface Science, 2006, 600, 4067-4071.	1.9	11
210	RHEED and XPS study of Pd–Sn bimetallic system growth. Surface Science, 2007, 601, 4475-4478.	1.9	11
211	Surface characterization of activated Ti–Zr–V NEG coatings. Vacuum, 2009, 83, 824-827.	3.5	11
212	Ptâ€doped tungsten oxide surface: photoemission and RHEED study. Surface and Interface Analysis, 2010, 42, 540-544.	1.8	11
213	Synchrotron radiation photoelectron spectroscopy studies of self-organization in As40Se60 nanolayers stored under ambient conditions and after laser irradiation. Journal of Non-Crystalline Solids, 2012, 358, 2910-2916.	3.1	11
214	Practical chemical analysis of Pt and Pd based heterogeneous catalysts with hard X-ray photoelectron spectroscopy. Journal of Electron Spectroscopy and Related Phenomena, 2013, 190, 268-277.	1.7	11
215	Photoemission study of cerium silicate model systems. Applied Surface Science, 2013, 265, 817-822.	6.1	11
216	The Mechanism of Hydrocarbon Oxygenate Reforming: CC Bond Scission, Carbon Formation, and Nobleâ€Metalâ€Free Oxide Catalysts. ChemSusChem, 2014, 7, 77-81.	6.8	11

#	Article	IF	CITATIONS
217	Redox-mediated conversion of atomically dispersed platinum to sub-nanometer particles. Journal of Materials Chemistry A, 2017, 5, 9250-9261.	10.3	11
218	Atomic Ordering and Sn Segregation in Pt–Sn Nanoalloys Supported on CeO2 Thin Films. Topics in Catalysis, 2017, 60, 522-532.	2.8	11
219	Nanoscale Morphological and Structural Transformations of PtCu Alloy Electrocatalysts during Potentiodynamic Cycling. Journal of Physical Chemistry C, 2018, 122, 21974-21982.	3.1	11
220	Selective electrooxidation of 2-propanol on Pt nanoparticles supported on Co ₃ O ₄ : an in-situ study on atomically defined model systems. Journal Physics D: Applied Physics, 2021, 54, 164002.	2.8	11
221	Investigation of Growth Mechanism of Thin Sputtered Cerium Oxide Films on Carbon Substrates. Science of Advanced Materials, 2014, 6, 1278-1285.	0.7	11
222	A photoemission study of the ceria and Au-doped ceria/Cu(111) interfaces. Vacuum, 2009, 84, 8-12.	3.5	10
223	Laser induced changes of As50Se50 nanolayers studied by synchrotron radiation photoelectron spectroscopy. Thin Solid Films, 2012, 520, 7224-7229.	1.8	10
224	Study of the character of gold nanoparticles deposited onto sputtered cerium oxide layers by deposition-precipitation method: Influence of the preparation parameters. Vacuum, 2015, 114, 86-92.	3.5	10
225	Dynamical Solvent Effects on the Charge and Reactivity of Ceria-Supported Pt Nanoclusters. Journal of Physical Chemistry C, 2018, 122, 27507-27515.	3.1	10
226	Perovskite ferroelectric thin film as an efficient interface to enhance the photovoltaic characteristics of Si/SnO _x heterojunctions. Journal of Materials Chemistry A, 2020, 8, 11314-11326.	10.3	10
227	First stages of the InP(1 0 0) surfaces nitridation studied by AES, EELS and EPES. Applied Surface Science, 2003, 212-213, 601-606.	6.1	9
228	Low pressure oxidation of ordered Sn/Pd(110) surface alloys. Journal of Physics Condensed Matter, 2009, 21, 185011.	1.8	9
229	Au-CeO2 nanoporous films/carbon nanotubes composites prepared by magnetron sputtering. Applied Surface Science, 2013, 267, 150-153.	6.1	9
230	In situ investigations of laser and thermally modified As2S3 nanolayers: Synchrotron radiation photoelectron spectroscopy and density functional theory calculations. Journal of Applied Physics, 2015, 118, .	2.5	9
231	Heteroepitaxy of Cerium Oxide Thin Films on Cu(111). Materials, 2015, 8, 6346-6359.	2.9	9
232	Inâ€Situ Investigation of Methane Dry Reforming on Metal/Ceria(111) Surfaces: Metal–Support Interactions and Câ^'H Bond Activation at Low Temperature. Angewandte Chemie, 2017, 129, 13221-13226.	2.0	9
233	Highly developed nanostructuring of polymer-electrolyte membrane supported catalysts for hydrogen fuel cell application. Journal of Power Sources, 2019, 439, 227084.	7.8	9
234	Effect of Cationic Interface Defects on Band Alignment and Contact Resistance in Metal/Oxide Heterojunctions. Advanced Electronic Materials, 2020, 6, 1900808.	5.1	9

#	Article	IF	CITATIONS
235	Nanoscale architecture of ceria-based model catalysts: Pt–Co nanostructures on well-ordered CeO2(111) thin films. Chinese Journal of Catalysis, 2020, 41, 985-997.	14.0	9
236	Investigation of dextran adsorption on polycrystalline cerium oxide surfaces. Applied Surface Science, 2021, 544, 148890.	6.1	9
237	Static SIMS investigation on Pd(111) surface during a catalytic reaction: CO oxidation. Surface Science, 1985, 162, 354-360.	1.9	8
238	Nitridation of InP(1 0 0) surface studied by AES and EELS spectroscopies. Vacuum, 2001, 63, 229-232.	3.5	8
239	Surface modification of GaAs during argon ionic cleaning and nitridation: EELS, EPES and XPS studies. Surface Science, 2004, 566-568, 1158-1162.	1.9	8
240	A photoelectron spectroscopy study of ultra-thin epitaxial alumina layers grown on Cu(111) surface. Surface Science, 2010, 604, 2073-2077.	1.9	8
241	Growth of thin epitaxial alumina films onto Ni(111): an electron spectroscopy and diffraction study. Surface and Interface Analysis, 2010, 42, 1581-1584.	1.8	8
242	Hydrogen activation on Pt–Sn nanoalloys supported on mixed Sn–Ce oxide films. Physical Chemistry Chemical Physics, 2014, 16, 13209.	2.8	8
243	Local surface structure and structural properties of As–Se nanolayers studied by synchrotron radiation photoelectron spectroscopy and DFT calculations. Journal of Non-Crystalline Solids, 2015, 410, 180-185.	3.1	8
244	Functionalization of nanostructured cerium oxide films with histidine. Physical Chemistry Chemical Physics, 2015, 17, 2770-2777.	2.8	8
245	Enhanced absorption of TiO ₂ nanotubes by N-doping and CdS quantum dots sensitization: insight into the structure. RSC Advances, 2018, 8, 35073-35082.	3.6	8
246	Adsorption structure of adenine on cerium oxide. Applied Surface Science, 2020, 530, 147257.	6.1	8
247	RHEED Study of Pd Particle Growth on α-Alumina and NaCl Substrates. Surface Review and Letters, 1998, 05, 403-408.	1.1	7
248	Pd Interaction with Reduced Thin-Film Alumina: XPS and ISS Study. Journal of Catalysis, 2001, 204, 372-377.	6.2	7
249	Sims study of Ti–Zr–V NEG thermal activation process. Vacuum, 2005, 80, 47-52.	3.5	7
250	Nitridation of InP(100) surface studied by synchrotron radiation. Surface Science, 2005, 583, 205-212.	1.9	7
251	Structure and electronic properties of gold adsorbed on Ti(0001). Applied Surface Science, 2006, 252, 5428-5431.	6.1	7
252	Refractory metal reactivity towards oxide surface: W/TiO2(1 1 0) case. Vacuum, 2007, 82, 146-149.	3.5	7

#	Article	IF	CITATIONS
253	XPS and TPD investigation of CO adsorption on mixed Rh–V layers supported by gamma-alumina. Applied Surface Science, 2011, 258, 908-913.	6.1	7
254	Nanoporous Pt ⁿ⁺ —CeO _{x catalyst films grown on carbon substrates. International Journal of Nanotechnology, 2012, 9, 680.}	0.2	7
255	Deposition of Pt and Sn doped CeOx layers on silicon substrate. Surface and Coatings Technology, 2013, 227, 15-18.	4.8	7
256	Epitaxial CeO2 thin films for a mechanism study of resistive random access memory (ReRAM). Journal of Solid State Electrochemistry, 2013, 17, 3137-3144.	2.5	7
257	Faceting Transition at the Oxide–Metal Interface: (13 13 1) Facets on Cu(110) Induced by Carpet-Like Ceria Overlayer. Journal of Physical Chemistry C, 2015, 119, 1851-1858.	3.1	7
258	Thermally Controlled Bonding of Adenine to Cerium Oxide: Effect of Substrate Stoichiometry, Morphology, Composition, and Molecular Deposition Technique. Journal of Physical Chemistry C, 2017, 121, 25118-25131.	3.1	7
259	Molecular beam study of CO chemisorption on alumina-supported Pd particles. European Physical Journal D, 1993, 43, 1023-1027.	0.4	6
260	Vacuum evaporation of thin alumina layers. Thin Solid Films, 1996, 289, 295-299.	1.8	6
261	Influence of Alumina Surface Structure on Growth and Adsorption Properties of Pd Particles. Surface Review and Letters, 1998, 05, 397-401.	1.1	6
262	Study of CO adsorption on Sn/Rh(111). Surface Science, 2007, 601, 3717-3721.	1.9	6
263	Structure of Pd/tungsten oxide epitaxial system. Vacuum, 2007, 82, 274-277.	3.5	6
264	The interfacial properties of MgCl2 thin films grown on Si(111)7×7. Journal of Chemical Physics, 2008, 128, 104705.	3.0	6
265	Growth of <scp>Al₂O₃</scp> Nanowires on the <scp>Cu</scp> â€9Âat.%Al(111) Single Crystal Surface. Journal of the American Ceramic Society, 2011, 94, 4084-4088.	3.8	6
266	Photoemission and RHEED study of the supported Pt and Au epitaxial alloy clusters. Applied Surface Science, 2013, 282, 746-756.	6.1	6
267	Model thin films of Ce(III)â€based mixed oxides. Surface and Interface Analysis, 2014, 46, 993-996.	1.8	6
268	Sol–gel preparation of alumina stabilized rare earth areo- and xerogels and their use as oxidation catalysts. Journal of Colloid and Interface Science, 2014, 422, 71-78.	9.4	6
269	Synchrotron XPS studies of illuminated and annealed flash evaporated a-Ge2S3 films. Journal of Non-Crystalline Solids, 2014, 401, 258-262.	3.1	6
270	RHEED structural study of the novel tin-cerium oxide catalyst. Ceramics International, 2015, 41, 4946-4952.	4.8	6

#	Article	IF	CITATIONS
271	Novel Fuel Cell MEA Based on Pt-C Deposited by Magnetron Sputtering. ECS Transactions, 2017, 80, 225-230.	0.5	6
272	Tailoring of highly porous SnO2 and SnO2-Pd thin films. Materials Chemistry and Physics, 2019, 232, 485-492.	4.0	6
273	Surface Composition of a Highly Active Pt ₃ Y Alloy Catalyst for Application in Low Temperature Fuel Cells. Fuel Cells, 2020, 20, 413-419.	2.4	6
274	Role of nitrogenated carbon in tuning Pt-CeOx based anode catalysts for higher performance of hydrogen-powered fuel cells. Applied Surface Science, 2020, 515, 146054.	6.1	6
275	TPD and static SIMS investigation of CO adsorption on Pd(111) during catalytic oxidation. Vacuum, 1986, 36, 449-452.	3.5	5
276	Steady carbon formation during CO oxidation over small Pd particles: A static sims study. Surface Science Letters, 1987, 186, 541-547.	0.1	5
277	Carbon monoxide oxidation on small supported palladium particles: Oxygen and CO surface diffusion. European Physical Journal D, 1989, 39, 1429-1431.	0.4	5
278	Study of desorption activation energy on Rh-CO systems. European Physical Journal D, 1993, 43, 957-961.	0.4	5
279	Photoelectron Spectroscopy Characterization of Diamond-like Carbon Films. Applied Spectroscopy, 2006, 60, 936-940.	2.2	5
280	Photoelectron spectroscopy and secondary ion mass spectrometry characterization of diamond-like carbon films. Thin Solid Films, 2007, 515, 5386-5390.	1.8	5
281	A photoemission study of carbon monoxide interaction with the Ga–Pd(110) system. Thin Solid Films, 2008, 517, 773-778.	1.8	5
282	Photoemission spectroscopy and electron diffraction study of Pd/tungsten oxide/W(110) epitaxial system. Journal of Physics: Conference Series, 2008, 100, 012008.	0.4	5
283	The interfacial properties of MgCl2 thin films grown on Ti(0001). Journal of Chemical Physics, 2010, 133, 074701.	3.0	5
284	Photoemission Study of Methanol Adsorption and Decomposition on Pd/CeO2(111)/Cu(111) Thin Film Model Catalyst. Catalysis Letters, 2015, 145, 1474-1482.	2.6	5
285	Structural and Chemical Characterization of Cerium Oxide Thin Layers Grown on Silicon Substrate. Materials Today: Proceedings, 2015, 2, 101-107.	1.8	5
286	Steering the formation of supported Pt–Sn nanoalloys by reactive metal–oxide interaction. RSC Advances, 2016, 6, 85688-85697.	3.6	5
287	Electrochemically shape-controlled transformation of magnetron sputtered platinum films into platinum nanostructures enclosed by high-index facets. Surface and Coatings Technology, 2017, 309, 6-11.	4.8	5
288	Annealing induced effect on the physical properties of ion-beam sputtered 0.5 Ba(Zr0.2Ti0.8)O3 –Â0.5 (Ba0.7Ca0.3)TiO3-δ ferroelectric thin films. Applied Surface Science, 2018, 443, 354-360.	6.1	5

#	Article	IF	CITATIONS
289	HfO ₂ –Al ₂ O ₃ Dielectric Layer for a Performing Metal–Ferroelectric–Insulator–Semiconductor Structure with a Ferroelectric 0.5Ba(Zr _{0.2} Ti _{0.8})O ₃ -0.5(Ba _{0.7} Ca _{0.3})TiO _{ Thin Film. ACS Applied Electronic Materials, 2020, 2, 2780-2787.}	34/3 3	5
290	The surface diffusion in CO oxidation on small supported Pd particles: Experimental evidence. Surface Science Letters, 1986, 166, L115-L118.	0.1	4
291	Structural model of CO dissociation on Pd particles. Zeitschrift Für Physik D-Atoms Molecules and Clusters, 1993, 26, 337-339.	1.0	4
292	Study of Al2O3 condensation on Si(100) and InP(100) substrates. Surface Science, 1996, 352-354, 407-410.	1.9	4
293	RHEED INVESTIGATION OF Pd/Al BIMETALLIC SYSTEM ON KCl(001) SUBSTRATE. Surface Review and Letters, 1999, 06, 825-828.	1.1	4
294	RHEED study of the growth of Pd–Al/MgO bimetallic system. Vacuum, 2005, 80, 102-107.	3.5	4
295	Angle-resolved photoemission of ordered <mmi:math xmlns:mml="http://www.w3.org/1998/Math/MathML" display="inline"><mml:mrow><mml:mi mathvariant="normal">Pb<mml:mo>â^•</mml:mo><mml:mi mathvariant="normal">Ni<mml:mrow><mml:mo>(</mml:mo><mml:mn>111</mml:mn><mml:mo>)<td>3.2 nml:mo≻∙</td><td>4 </td></mml:mo></mml:mrow></mml:mi </mml:mi </mml:mrow></mmi:math 	3.2 nml:mo≻∙	4
296	Combined EELS, LEED and SR-XPS study of ultra-thin crystalline layers of indium nitride on InP(100)—Effect of annealing at 450ŰC. Applied Surface Science, 2007, 253, 4445-4449.	6.1	4
297	Photoemission study of methanol decomposition on Pt/Ni(111) surface alloy. Surface and Interface Analysis, 2010, 42, 555-558.	1.8	4
298	Position of segregated Al atoms and the work function: Experimental low energy electron diffraction intensity analysis and first-principles calculation of the (Ⱊ3×Ⱊ3)R30° superlattice phase on the (111) surface of a Cu–9at.%Al alloy. Journal of Vacuum Science and Technology A: Vacuum, Surfaces and Films, 2010, 28, 152-158.	2.1	4
299	The Influence of Vanadium Microalloying on Voids Occurence in Low-Alloyed Cr-Mo Steels After Continuous Casting. International Journal of Fracture, 2011, 168, 259-266.	2.2	4
300	Sn/Pt(110) bimetallic surfaces: formation and oxygen adsorption. Journal of Physics Condensed Matter, 2011, 23, 215002.	1.8	4
301	Bimetallic bonding and mixed oxide formation in the Ga–Pd–CeO2 system. Journal of Applied Physics, 2011, 110, 043726.	2.5	4
302	Mass Spectrometry of Polymer Electrolyte Membrane Fuel Cells. Journal of Analytical Methods in Chemistry, 2016, 2016, 1-9.	1.6	4
303	Histidine adsorption on nanostructured cerium oxide. Journal of Electron Spectroscopy and Related Phenomena, 2016, 212, 28-33.	1.7	4
304	Exploiting micro-scale structural and chemical observations in real time for understanding chemical conversion: LEEM/PEEM studies over CeOx–Cu(111). Ultramicroscopy, 2017, 183, 84-88.	1.9	4
305	Influence of chemical equilibrium in introduced oxygen vacancies on resistive switching in epitaxial Pt-CeO2 system. Journal of Solid State Electrochemistry, 2017, 21, 657-664.	2.5	4
306	Super-bandgap light stimulated reversible transformation and laser-driven mass transport at the surface of As2S3 chalcogenide nanolayers studied <i>in situ</i> . Journal of Chemical Physics, 2018, 149, 214702.	3.0	4

#	Article	IF	CITATIONS
307	Reversible structural changes of in situ prepared As40Se60 nanolayers studied by XPS spectroscopy. Applied Nanoscience (Switzerland), 2019, 9, 917-924.	3.1	4
308	Characterization of innovative Pt-ceria catalysts for PEMFC by means of ex-situ and operando X-Ray Absorption Spectroscopy. International Journal of Hydrogen Energy, 2022, 47, 8799-8810.	7.1	4
309	Catalytic activity of small supported Pd/Al2O3 particles: CO oxidation. Zeitschrift Für Physik D-Atoms Molecules and Clusters, 1988, 10, 499-501.	1.0	3
310	Rheed study of Pd particle growth on insulator substrates. European Physical Journal D, 1993, 43, 881-885.	0.4	3
311	Electron elastic scattering study of thin film growth mode: Rh on Al2O3. Vacuum, 1998, 50, 147-149.	3.5	3
312	SSIMS and XPS Studies of Reconstruction of Alumina-Supported Rh Particles. Surface Review and Letters, 1998, 05, 375-379.	1.1	3
313	Auger electronic spectroscopy and electrical characterisation of InP(100) surfaces passivated by N2 plasma. Applied Surface Science, 2004, 234, 451-456.	6.1	3
314	Passivation of InP(100) substrates: first stages of nitridation by thin InN surface overlayers studied by electron spectroscopies. Surface and Interface Analysis, 2005, 37, 615-620.	1.8	3
315	Interaction of CO with Palladium Supported on Oxidized Tungsten. Journal of Physical Chemistry B, 2006, 110, 23837-23844.	2.6	3
316	Photoemission study of the (2×2) structure formed by H2O adsorption on the Zr(0001) surface. Surface Science, 2006, 600, 3581-3585.	1.9	3
317	Interaction of ethylene with palladium clusters supported on oxidised tungsten foil. Surface Science, 2007, 601, 3114-3124.	1.9	3
318	Photoelectron-spectroscopic and reactivity investigation of thin Pd–Sn films prepared by magnetron sputtering. Applied Surface Science, 2007, 253, 5400-5403.	6.1	3
319	The growth of Au/Pd/alumina/Cu–Al system studied by SRPES. Applied Surface Science, 2008, 254, 4340-4345.	6.1	3
320	Core level photoemission and STM characterization of Ta/Si(111)-7×7 interfaces. Surface Science, 2009, 603, 469-476.	1.9	3
321	Excitons at the B K edge of boron nitride nanotubes probed by x-ray absorption spectroscopy. Journal of Physics Condensed Matter, 2010, 22, 295301.	1.8	3
322	Interaction of oxygen with Au/Ti(0001) surface alloys studied by photoelectron spectroscopy. Journal of Physics Condensed Matter, 2010, 22, 265002.	1.8	3
323	Two-dimensional, high valence-doped ceria: Ce 6 WO 12 (100)/W(110). Applied Surface Science, 2016, 372, 152-157.	6.1	3
324	The influence of Si in Ni on the interface modification and the band alignment between Ni and alumina. Applied Surface Science, 2018, 442, 164-169.	6.1	3

#	Article	IF	CITATIONS
325	Study of palladium interaction with magnetron sputtered SnO2 films. E-Journal of Surface Science and Nanotechnology, 2006, 4, 497-503.	0.4	3
326	Steady carbon formation during CO oxidation over small Pd particles: A static SIMS study. Surface Science Letters, 1987, 186, L541-L547.	0.1	2
327	UHV aluminium oxide on silicon substrates: electron spectroscopies analysis and electrical measurements. Applied Surface Science, 2001, 175-176, 656-662.	6.1	2
328	Study of the growth of supported Pd–Sn bimetallic nanoclusters. Thin Solid Films, 2006, 515, 563-566.	1.8	2
329	A valence band photoemission study of Pb adsorption on Rh(1 0 0) and Rh(1 1 0). Surface Science, 2007, 601, 5673-5677.	1.9	2
330	XPS and LEED study of Pd and Au growth on alumina/Cu–Al surface. Applied Surface Science, 2007, 254, 490-493.	6.1	2
331	Electronic exchanges between adsorbed Ni atoms and TiO2(110) surface evidenced by resonant photoemission. Journal of Electron Spectroscopy and Related Phenomena, 2011, 184, 410-413.	1.7	2
332	Photoemission and LEED study of the Sn/Rh(111) surface—early oxidation steps and thermal stability. Journal of Physics Condensed Matter, 2012, 24, 015002.	1.8	2
333	Adsorption of ethylene on Sn and In terminated Si(001) surface studied by photoelectron spectroscopy and scanning tunneling microscopy. Journal of Chemical Physics, 2016, 145, 094701.	3.0	2
334	Growth of cerium tungstate epitaxial layers: influence of temperature. Surface and Interface Analysis, 2016, 48, 111-114.	1.8	2
335	On the growth mechanisms of polar (100) surfaces of ceria on copper (100). Surface Science, 2018, 671, 1-5.	1.9	2
336	Pt–CeO2 Catalysts for Fuel Cell Applications: From Surface Science to Electrochemistry. , 2018, , 189-201.		2
337	Monte Carlo simulation of catalytic CO oxidation. Progress in Surface Science, 1990, 35, 193-196.	8.3	1
338	Reactivity of small supported particles. European Physical Journal D, 1993, 43, 947-951.	0.4	1
339	CO adsorption on Pd particles: TDS studies. European Physical Journal D, 1993, 43, 769-776.	0.4	1
340	The RHEED and ESDIAD methods as a probe of supported particle structure and morphology: Pd on KCl. Surface Science, 1994, 321, L143-L148.	1.9	1
341	Structural study of epitaxial tungsten oxide nanoclusters. Vacuum, 2005, 80, 58-63.	3.5	1
342	Fermi surface and band mapping of the cerium/palladium surface alloy. Surface Science, 2007, 601, 4058-4062.	1.9	1

#	Article	IF	CITATIONS
343	The growth of Au/Pd on alumina/Cu-Al system. Journal of Physics: Conference Series, 2008, 100, 012040.	0.4	1
344	Intra-atomic charge re-organization at the Pb–Si interface: Bonding mechanism at low coverage. Surface Science, 2009, 603, 2861-2869.	1.9	1
345	Investigation of the Ti/MgCl2 interface on a Si(111) 7 × 7 substrate. Journal of Chemical Physics, 2012, 136, 224703.	3.0	1
346	Depth profiling of ultra-thin alumina layers grown on Co(0001). Journal of Physics Condensed Matter, 2013, 25, 095004.	1.8	1
347	The effect of the substrate on thermal stability of CeO <i>_x</i> and Rh–Ce–O thin films. Surface and Interface Analysis, 2014, 46, 980-983.	1.8	1
348	Evidence for two growth modes during tungsten oxide vapor deposition on mica substrates. Journal of Crystal Growth, 2014, 394, 67-73.	1.5	1
349	Catalytic activity of small supported Pd/Al2O3 particles: CO oxidation. Zeitschrift Für Physik D-Atoms Molecules and Clusters, 1989, 13, 77-77.	1.0	Ο
350	A RHEED and AFM study of the epitaxial growth of Pd on Pd(001). European Physical Journal D, 1995, 45, 777-784.	0.4	0
351	Associative electron stimulated desorption of neutral CO molecules. European Physical Journal D, 2001, 51, 1229-1235.	0.4	Ο
352	Surface alloying in the Sn/Ni(111) system studied by synchrotron radiation photoelectron valence band spectroscopy and ab-initio density of states calculations. Thin Solid Films, 2008, 516, 2962-2965.	1.8	0
353	Electronic and adsorption properties of Ceâ€Ag layers. Surface and Interface Analysis, 2011, 43, 1539-1542.	1.8	Ο
354	Comment to: "Meliorated oxygen reduction reaction of polymer electrolyte membrane fuel cell in the presence of cerium–zirconium oxide―by B. Yamini Sarada, K.S. Dhathathreyan, and M. Rama Krishna. International Journal of Hydrogen Energy, 2012, 37, 5307-5308.	7.1	0
355	X-ray small-angle scattering from sputtered CeO2/C bilayers. Journal of Applied Physics, 2013, 113, 024301.	2.5	0
356	Influence of external factors on optical parameters in Cu ₆ PS ₅ I thin films. Proceedings of SPIE, 2015, , .	0.8	0
357	Growth of transition metals on cerium tungstate model catalyst layers. Journal of Physics Condensed Matter, 2016, 28, 395002.	1.8	0
358	CeOx(111)/Cu(111) Thin Films as Model Catalyst Supports. Springer Series in Materials Science, 2016, , 233-250.	0.6	0
359	Thin Film Catalysts for Proton Exchange Membrane Fuel Cells. , 2018, , 351-359.		0
360	Reversible laser-assisted structural modification of the surface of As-rich nanolayers for active photonics media. Applied Surface Science, 2020, 518, 146240.	6.1	0

#	Article	IF	CITATIONS
361	Fiber-like Structure on the Proton Exchange Membrane Created By Simultaneous Magnetron Sputtering and Plasma Etching in Role of a Catalyst Support in Water Electrolyzers. ECS Meeting Abstracts, 2020, MA2020-01, 1586-1586.	0.0	0